First Measurement of the Decay Dynamics in the Semileptonic Transition of $D^{+(0)}$ into the Axial-Vector Meson $\bar{K}_1(1270)$

M. Ablikim *et al.*[*]
(BESIII Collaboration)

(Received 3 March 2025; revised 24 July 2025; accepted 29 July 2025; published 25 August 2025)

Using e^+e^- data taken at the center-of-mass energy of 3.773 GeV with the BESIII detector, corresponding to an integrated luminosity of 20.3 fb^{-1}, we report the first measurement of the decay dynamics of the semileptonic decays $D^{+(0)} \to K^-\pi^+\pi^{0(-)}e^+\nu_e$. The amplitude analysis gives the hadronic form factors of the semileptonic D transitions into the axial-vector meson $\bar{K}_1(1270)$ to be $r_A = (-11.2 \pm 1.0_{\rm stat} \pm 0.9_{\rm syst}) \times 10^{-2}$ and $r_V = (-4.3 \pm 1.0_{\rm stat} \pm 2.5_{\rm syst}) \times 10^{-2}$. This is the first in the semileptonic decays of heavy mesons into axial-vector mesons. The angular analysis yields an up-down asymmetry $\mathcal{A}'_{\rm ud} = 0.01 \pm 0.11$, which is consistent with the standard model prediction. In addition, the branching fractions of $D^+ \to \bar{K}_1(1270)^0 e^+\nu_e$ and $D^0 \to K_1(1270)^- e^+\nu_e$ are determined with improved precision to be $(2.27 \pm 0.11_{\rm stat} \pm 0.07_{\rm syst} \pm 0.07_{\rm input}) \times 10^{-3}$ and $(1.02 \pm 0.06_{\rm stat} \pm 0.06_{\rm syst} \pm 0.03_{\rm input}) \times 10^{-3}$, respectively. No significant signals of $D^+ \to \bar{K}_1(1400)^0 e^+\nu_e$ and $D^0 \to K_1(1400)^- e^+\nu_e$ are observed and their branching fraction upper limits are set as 1.4×10^{-4} and 0.7×10^{-4} at 90% confidence level, respectively.

DOI: 10.1103/xj42-xgzf

The partial decay rates of semileptonic (SL) D decays are usually decomposed as functions of the quark mixing matrix element $|V_{cs}|$ or $|V_{cd}|$ [1,2] and the hadronic form factors (FFs) describing strong interaction effects binding quarks into hadrons. Over the past few decades, the hadronic FFs of the SL D decays into S-wave states (pseudoscalar or vector mesons) have been precisely and extensively studied in theory [3] and experiment [4,5]. However, there is scant information regarding the SL decay of D into P-wave states. As a Cabibbo-favored transition into the lowest lying axial-vector meson octet, the $D \to \bar{K}_1(1270)$ transition is expected to be the most promising channel with significantly higher statistics. There have been some model predictions on its hadronic FFs [6–10], but no experimental information yet.

In theory, the physical mass eigenstates of the strange axial-vector mesons, $K_1(1270)$ and $K_1(1400)$, are a mixture of the $^1P_1$ and $^3P_1$ states with a mixing angle θ_{K_1}. Some theoretical calculations of the hadronic FFs of $D \to \bar{K}_1(1270)$ have come from light-cone QCD sum rules [6], three-point QCD sum rules (3PSR) [7], AdS/QCD [8], and covariant light front approach [9,10]. The predicted FFs are in wide range due to being sensitive to both the theoretical approaches and θ_{K_1}. However, the value of θ_{K_1} is still very controversial in various phenomenological analyses of different processes [11–19]. Experimental measurements of the hadronic FFs of $D \to \bar{K}_1(1270)$ are crucial to test different theoretical calculations, and thereby restrict the θ_{K_1}. A verified θ_{K_1} value is key to guide the theoretical calculations of different decays of τ [12], B [14,20], and D [21,22] particles into strange axial-vector mesons.

Additionally, Refs. [23,24] state that the analysis of $B \to K_1(1270)\gamma$ when combined with $D^{0(+)} \to \bar{K}_1(1270)\ell^+\nu_\ell$ offers a potential way to extract photon polarization in $b \to s\gamma$ transitions without considerable theoretical ambiguity. The improved knowledge of photon polarization in $b \to s\gamma$ transitions is powerful to probe right-handed couplings in new physics [25–27]. Previously, a significant photon polarization was observed in the $B^+ \to K_1(1270)^+(\to K^+\pi^-\pi^+)\gamma$ decay by measuring its up-down asymmetry $\mathcal{A}_{\rm ud} = f_h\lambda_\gamma$ [28]. Therefore, determination of the up-down asymmetry $\mathcal{A}'_{\rm ud}$ in the SL decays $D^{+(0)} \to \bar{K}_1(1270)^{0(-)}(\to K^-\pi^+\pi^{0(-)})e^+\nu_e$, is highly desired to quantify the hadronic effects of $K_1(1270)^- \to K^-\pi^+\pi^-$ with $f_h = \frac{3}{4}\mathcal{A}'_{ud}$.

Previously, only CLEO and BESIII reported the branching fraction (BF) measurements of $D^{+(0)} \to \bar{K}_1(1270)^{0(-)}e^+\nu_e$ [29–32]. This Letter reports the first determinations of the hadronic FFs of $D \to \bar{K}_1(1270)$ (r_A and r_V) and up-down asymmetry ($\mathcal{A}'_{\rm ud}$), using 20.3 fb^{-1} of

[*]Full author list given at the end of the Letter.

e^+e^- data [33] collected by BESIII at $\sqrt{s} = 3.773$ GeV. Improved measurements of the BFs of $D \to \bar{K}_1(1270)e^+\nu_e$ and the first search for $D \to \bar{K}_1(1400)e^+\nu_e$ are also presented [34].

Details about the design and performance of the BESIII detector are given in Refs. [35,36]. The inclusive Monte Carlo (MC) samples, described in Refs. [37–42], are used to model the background in this analysis. The signal MC samples of the $D^{+(0)} \to K^-\pi^+\pi^{0(-)}e^+\nu_e$ decay are generated based on the amplitude analysis result obtained in this Letter.

At $\sqrt{s} = 3.773$ GeV, the D and $\bar{D}$ mesons are produced in pairs without accompanying particles in the final state; this allows us to study SL D decays with the double-tag (DT) method [43]. The single-tag (ST) $\bar{D}$ mesons are reconstructed with the hadronic decay modes $\bar{D}^0 \to K^+\pi^-, K^+\pi^-\pi^0$, and $K^+\pi^-\pi^-\pi^+$; $D^- \to K^+\pi^-\pi^-, K^0_S\pi^-$, $K^+\pi^-\pi^-\pi^0, K^0_S\pi^-\pi^0, K^0_S\pi^+\pi^-\pi^-$, and $K^+K^-\pi^-$. In the presence of the ST $\bar{D}$ mesons, candidates for the signal decays $D^{+(0)} \to K^-\pi^+\pi^{0(-)}e^+\nu_e$ are selected to form DT events. The BF of the signal decay is determined by

$$\mathcal{B}_{\rm sig} = \frac{N^{\rm sig}_{\rm DT}}{N^{\rm tot}_{\rm ST}\bar{\epsilon}_{\rm sig}}, \tag{1}$$

where $N^{\rm tot}_{\rm ST} = \sum_i N^i_{\rm ST}$ and $N^{\rm sig}_{\rm DT}$ are the total ST and DT yields after summing over all tag modes; $\bar{\epsilon}_{\rm sig} = \sum_i (N^i_{\rm ST}/N^{\rm tot}_{\rm ST})(\epsilon^i_{\rm DT}/\epsilon^i_{\rm ST})$ is the averaged signal efficiency of selecting $D^{+(0)} \to K^-\pi^+\pi^{0(-)}e^+\nu_e$ in the presence of the ST $\bar{D}$ mesons, where $\epsilon^i_{\rm ST}$ and $\epsilon^i_{\rm DT}$ are the ST and DT efficiencies for the ith tag mode, respectively.

The selection criteria for $\pi^\pm, K^\pm, K^0_S, \gamma$, and π^0 candidates are the same as Ref. [43]. Two kinematic variables, the energy difference $\Delta E \equiv E_{\bar{D}} - E_{\rm beam}$ and the beam-constrained mass $M_{\rm BC} \equiv \sqrt{E^2_{\rm beam} - |\vec{p}_{\bar{D}}|^2}$, are used to distinguish the ST $\bar{D}$ mesons from the combinatorial background, where $E_{\rm beam}$ is the beam energy and $(E_{\bar{D}}, \vec{p}_{\bar{D}})$ is the four-momentum of ST $\bar{D}$ in the e^+e^- rest frame. The combination with the smallest $|\Delta E|$ is chosen if there are multiple combinations in the event.

The ST candidates are required to satisfy the tag mode requirements of ΔE, corresponding to about $\pm 3.5\sigma$ around the fitted peaks. The ST yields in data for each tag mode are extracted by fitting individual $M_{\rm BC}$ distributions. Candidates with $M_{\rm BC} \in [1.859, 1.873]$ GeV/c^2 for $\bar{D}^0$ and $M_{\rm BC} \in [1.863, 1.877]$ GeV/c^2 for D^- are retained for further analysis. The ΔE requirements, the ST yields in data, and the ST efficiencies for different tag modes are provided in Ref. [44]. Summing over all tag modes gives $N^{\rm tot}_{\rm ST}$ to be $(10677.9 \pm 3.8) \times 10^3$ for D^- and $(16146.2 \pm 4.6) \times 10^3$ for $\bar{D}^0$.

In the presence of the tagged $\bar{D}$, candidates for $D^{+(0)} \to K^-\pi^+\pi^{0(-)}e^+\nu_e$ are selected from the residual tracks and showers. The selection criteria of K^-, $\pi^\pm$, and π^0 candidates are the same as those used in the ST selection. The e^+ candidates are selected by performing particle identification (PID) based on the specific ionization energy loss dE/dx, time of flight, and electromagnetic calorimeter information. Confidence levels (CL) for the positron, pion, and kaon hypotheses, denoted as $\mathrm{CL}_{e,\pi,K}$, are calculated. Charged tracks are assigned as e^+ candidates if $\mathrm{CL}_e > 0.001$ and $\mathrm{CL}_e/(\mathrm{CL}_e + \mathrm{CL}_\pi + \mathrm{CL}_K) > 0.8$. To further distinguish the positron candidates from hadrons, the e^+ candidates are required to satisfy $E/p - 0.05 \times \chi^2_{e-dE/dx} > 0.53$ and 0.60 for D^+ and D^0 channels, respectively. Here, E is the deposited energy in the electromagnetic calorimeter, p is the momentum measured by the drift chamber, and $\chi^2_{e-dE/dx}$ is the χ^2 with the positron hypothesis based on the dE/dx information. To partially recover the energy loss due to final state radiation for positrons, the neutral showers within 5° of the initial positron direction are merged to the four-momentum of the positron measured by the drift chamber. No additional charged tracks are allowed in the event to suppress the hadronic background.

Since the neutrino cannot be detected by the BESIII detector, its four-momentum $(E_{\rm miss}, \vec{p}_{\rm miss})$ is obtained by calculating the missing energy and momentum, defined as $E_{\rm miss} \equiv E_{\rm beam} - \sum_j E_j$ and $\vec{p}_{\rm miss} \equiv \vec{p}_D - \sum_j \vec{p}_j$. Here, the index j sums over the $K^-, \pi^+, \pi^{0(-)}$, and e^+ of the signal candidates and $(E_j, \vec{p}_j)$ is the four-momentum of the jth particle. A kinematic variable $U_{\rm miss} \equiv E_{\rm miss} - |\vec{p}_{\rm miss}|$ is defined to extract the signal yield. To further improve the resolutions of the above variables, the momentum of the D meson is constrained as $\vec{p}_D = -\hat{p}_{\bar{D}}\sqrt{E^2_{\rm beam} - m^2_{\bar{D}}}$, where $\hat{p}_{\bar{D}}$ is the unit vector in the momentum direction of the ST $\bar{D}$ meson and $m_{\bar{D}}$ is the known $\bar{D}$ mass [48].

Further requirements are applied to veto the background following Refs. [30,31]. For the D^+ channel, the momentum of the π^0 candidate must be greater than 0.2 GeV/c to suppress the fake π^0 candidates; the invariant mass of $K^-\pi^+\pi^0e^+$ is required to be less than 1.78 GeV/c^2 to reject the hadronic decay $D^+ \to K^-\pi^+\pi^0\pi^+$; to suppress the background from $D^+ \to K^-\pi^+e^+\nu_e$ with a fake π^0, the $U'_{\rm miss}$ variable is calculated by ignoring the π^0, and events with $U'_{\rm miss} < 0.03$ GeV are rejected. For the D^0 channel, the invariant mass of $K^-\pi^+\pi^-\pi^+_{e\to\pi}$ is required to be less than 1.80 GeV/c^2 to reject the hadronic decay $D^0 \to K^-\pi^+\pi^-\pi^+$, where $\pi^+_{e\to\pi}$ is obtained by replacing the energy of the e^+ track with the pion mass; the opening angle between e^+ and π^- is required to satisfy $\cos\theta_{e^+\pi^-} < 0.93$ to suppress the background from $D^0 \to K^-\pi^+\pi^0(\pi^0), \pi^0 \to e^+e^-\gamma$ with e^- misidentified as π^-; the background $D^0 \to K^-\pi^+\pi^-\pi^+\pi^0$ is suppressed by requiring $\cos(\nu_e, \gamma) < 0.78$, where γ is the most energetic extra photon; the background from $D^0 \to K^-\pi^0e^+\nu_e, \pi^0 \to e^+e^-\gamma$ with e^+e^- misidentified as $\pi^+\pi^-$ is rejected by

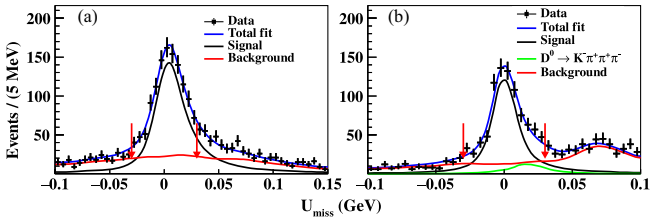

FIG. 1. Fits to the $U_{\rm miss}$ distributions of the (a) D^+ and (b) D^0 channels. The points with error bars are data. The blue solid lines denote the total fits. The black, green, and red lines show the signal, peaking background, and nonpeaking background contributions, respectively. The pairs of red arrows indicate the requirement $|U_{\rm miss}| < 0.03$ GeV.

requiring the $\pi^+\pi^-$ invariant mass to be less than 0.31 GeV/c^2; events with $D^- \to K^+\pi^-\pi^-$ versus $D^+ \to \pi^0 X$ can be potentially reconstructed as the tag mode $\bar{D}^0 \to K^+\pi^-\pi^0$, and are suppressed by requiring $|\Delta E[(K^+\pi^-)_{\rm tag}\pi^-_{\rm sig}]| > 7$ MeV.

To extract the signal yields of $D^{+(0)} \to K^-\pi^+\pi^{0(-)}e^+\nu_e$, unbinned maximum likelihood fits are performed on the $U_{\rm miss}$ distributions of the accepted candidates, as shown in Fig. 1. In the fit, the signal is modeled by the MC-simulated shape convolved with a Gaussian function with free parameters, and the background shape is derived from the inclusive MC sample. For the D^0 channel, the peaking background $D^0 \to K^-\pi^+\pi^-\pi^+$ is modeled based on the amplitude analysis result [49] with fixed yield according to the simulated sample, while the yield of the other background components is allowed to float. There is no significant peaking background for the D^+ channel and the yield of all the background contributions is allowed to float. The signal efficiencies are estimated based on the signal MC samples generated with the amplitude analysis result. The fitted signal yields from the data, the averaged signal efficiencies, and the obtained BFs are summarized in Table I.

Events satisfying $|U_{\rm miss}| < 0.03$ GeV are kept for the amplitude analysis. In total 1226 and 882 data candidates for the D^+ and D^0 channels survive with background fractions of $(21.9 \pm 1.4)\%$ and $(26.7 \pm 1.4)\%$, respectively. In the amplitude analysis, the covariant tensor amplitude is constructed as

TABLE I. Fitted signal yields in data ($N^{\rm sig}_{\rm DT}$), averaged signal efficiencies ($\bar{\epsilon}_{\rm sig}$), and obtained BFs ($\mathcal{B}_{\rm sig}$), where the first uncertainties are statistical and the second systematic.

Channel	$N^{\rm sig}_{\rm DT}$	$\bar{\epsilon}_{\rm sig}$ (%)	$\mathcal{B}_{\rm sig}(\times 10^{-3})$
D^+	1270 ± 56	9.45 ± 0.02	$1.27 \pm 0.06 \pm 0.04$
D^0	731 ± 35	14.12 ± 0.03	$0.32 \pm 0.02 \pm 0.02$

$$\mathcal{M} = (V-A)^{\mu\eta} \cdot \left[\sum_{\lambda_W} \epsilon^*(\lambda_W)_\mu \epsilon(\lambda_W)_\rho\right] \cdot \left[\sum_{\lambda_{K_1}} \epsilon^*(\lambda_{K_1})_\eta \epsilon(\lambda_{K_1})_\sigma\right] \cdot \mathcal{R}_{\bar{K}_1} \cdot J^\sigma \cdot \bar{u}_\nu \gamma^\rho (1-\gamma_5) v_l. \tag{2}$$

Here, $(V-A)^{\mu\eta}\epsilon^*(\lambda_{K_1})_\eta$ is the current for $D \to \bar{K}_1 W^*$ following the convention in Ref. [24], written as

$$\begin{aligned} V^{\mu\eta}\epsilon^*(\lambda_{K_1})_\eta &= -(m_D - M_{K_1})V_1(q^2)\epsilon^{*\mu}(\lambda_{K_1}) \\ &\quad + V_2(q^2)\left(\frac{q\cdot\epsilon^*(\lambda_{K_1})}{m_D - M_{K_1}}\right)(p_D + p_{K_1})^\mu, \\ A^{\mu\eta}\epsilon^*(\lambda_{K_1})_\eta &= -\frac{2iA(q^2)}{m_D - M_{K_1}}\epsilon^{\mu\epsilon^*(\lambda_{K_1})p^D p^{K_1}}. \end{aligned} \tag{3}$$

Both vector and axial-vector FFs take single pole form, written as $V_{1,2}(q^2) = [V_{1,2}(0)/(1 - q^2/m_V^2)]$ and $A(q^2) = [A(0)/(1 - q^2/m_A^2)]$ with $q^\mu = p_D^\mu - p_{K_1}^\mu$. More sophisticated parametrizations [50,51] are discussed as shown in Appendix A; $\epsilon(\lambda_W)$ and $\epsilon(\lambda_{K_1})$ are the polarization vectors of the W boson and the $\bar{K}_1$ meson, respectively; $\mathcal{R}_{\bar{K}_1} = [1/(s - m_0^2 + im_0\Gamma_0)]$ is the Breit-Wigner function of $\bar{K}_1$ with mass m_0 and width Γ_0; J^σ is the hadronic current of $\bar{K}_1 \to K^-\pi^+\pi^{0(-)}$; $W^* \to e^+\nu_e$ is described with $\bar{u}_\nu\gamma^\rho(1-\gamma_5)v_l$. See more details about the amplitude formula in Ref. [44]. For the charge conjugate decay modes, the three-momenta of the final states from $\bar{D}$ decay are inverted to incorporate them with the D by assuming charge-parity conservation.

The log-likelihood function for this unbinned maximum likelihood fit is constructed as

$$\ln\mathcal{L} = \sum_k^{N_{\rm data}} \ln\left[(1-\omega_{\rm bkg})\frac{|\mathcal{M}(p_j^k)|^2}{\int\epsilon(p_j)|\mathcal{M}(p_j)|^2 R_5(p_j)\mathrm{d}p_j} + \omega_{\rm bkg}\frac{B_\epsilon(p_j^k)}{\int\epsilon(p_j)B_\epsilon(p_j)R_5(p_j)\mathrm{d}p_j}\right], \tag{4}$$

where $N_{\rm data}$ is the number of events in the data sample, $\omega_{\rm bkg}$ is the background fraction, p_j is the four-momentum of final states, B_ϵ is the background distribution corrected by acceptance. The integration over five-body phase space R_5 is calculated numerically [52] based on massive MC samples. A simultaneous fit is performed to D^+ and D^0 channels by summing over their log-likelihood functions. The isospin relationships are imposed to constrain the FFs in the SL decays and complex coupling coefficients in the hadronic current J^σ as shown in Ref. [44]. Here, $V_1(0)$ is fixed to be 1 with the ratio $r_V = [V_2(0)/V_1(0)]$ and $r_A = [A(0)/V_1(0)]$ allowed to float. The mass and width of $K_1(1270)$ are free in the fit.

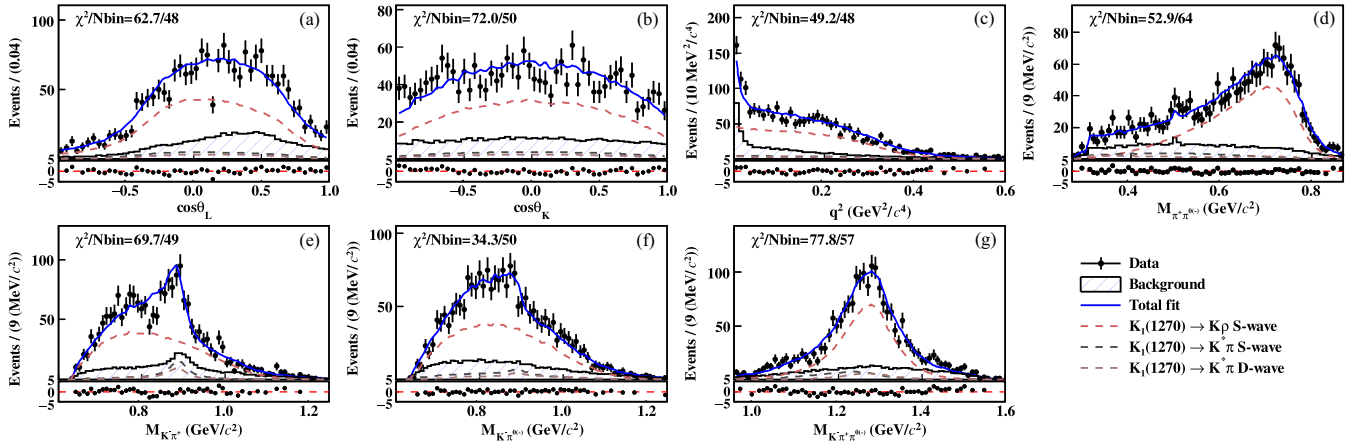

FIG. 2. Projections of the amplitude analysis result on (a) $\cos\theta_L$, (b) $\cos\theta_K$, (c) q^2, (d) $M_{\pi^+\pi^{0(-)}}$, (e) $M_{K^-\pi^+}$, (f) $M_{K^-\pi^{0(-)}}$, and (g) $M_{K^-\pi^+\pi^{0(-)}}$. The dots with error bars are data, the blue solid curves are the total fit results, the dashed curves represent the various components, and the blue hatched histograms are the simulated backgrounds derived from the inclusive MC sample. The pull distributions, defined as $\chi = (N_{\rm data} - N_{\rm fit})/\sqrt{N_{\rm fit}}$, are shown in the lower plots, where $N_{\rm data}$ and $N_{\rm fit}$ are the data and fit projection numbers of events for each bin, respectively.

Several potential substructures in $\bar{K}_1(1270) \to K^-\pi^+\pi^{0(-)}$, including $\rho, \bar{K}^*(892), \omega$, and $(\bar{K}\pi)_{S\text{-wave}}$, are considered in the significance test. The contribution from $\bar{K}_1(1400) \to \bar{K}^*(892)\pi$ is also tested, which yields statistical significance less than 3σ. The nominal solution is determined to include $\bar{K}_1(1270) \to \rho K^-$ (S wave) and $\bar{K}_1(1270) \to \pi\bar{K}^*(892)$ (S and D waves) with statistical significance greater than 5σ. Figure 2 shows the projections of the nominal fit result. The kinematic variable $\cos\theta_L$ is the angle between the vector opposite to the flight direction of D and e^+ in the W-boson rest frame; $\cos\theta_K$ is the angle between the vector opposite to the flight direction of D and the normal to the K_1 decay plane $\vec{n} = \vec{p}_{\pi^+} \times \vec{p}_{\pi^{0(-)}}$ in the $\bar{K}_1$ rest frame. The projections on helicity angles in the secondary decay $\bar{K}_1(1270) \to K^-\pi^+\pi^{0(-)}$ are presented in Appendix B. The fitted parameters and the fit fractions are summarized in Table II. Here, the fit fraction f_i of the ith component is determined with

$$f_i = \int |\mathcal{M}_i|^2 R_5(p_j)dp_j / \int |\mathcal{M}|^2 R_5(p_j)dp_j, \quad (5)$$

where $\mathcal{M}_i$ is the amplitude with the ith component's contribution only. The BF ratio of $\{\mathcal{B}[K_1(1270) \to K^*\pi]/\mathcal{B}[K_1(1270) \to K\rho]\}$ is calculated to be $(20.3 \pm 2.1_{\rm stat} \pm 8.7_{\rm syst})\%$, which is consistent with those derived from Refs. [53–55] but disfavors those obtained in Refs. [56,57]. Furthermore, with $\bar{K}_1(1400) \to \bar{K}^*(892)\pi$ involved in fit, the upper limit of corresponding fit fraction is set to be 9% for D^0 and 5% for D^+ at 90% CL.

By applying the isospin relationship and ignoring the insignificant contribution from $K_1(1270) \to K_0^*(1430)\pi$, the BFs of $\mathcal{B}(\bar{K}_1(1270)^0 \to K^-\pi^+\pi^0) = \mathcal{B}_{\rm 3body} \cdot [(3 + 4\alpha)/9(1 + \alpha)]$ and $\mathcal{B}(K_1(1270)^- \to K^-\pi^+\pi^-) = \mathcal{B}_{\rm 3body} \cdot [(6 + 4\alpha)/9(1 + \alpha)]$ are calculated to be $(56.0 \pm 1.7)\%$ and $(31.3 \pm 0.9)\%$, respectively. Here, $\mathcal{B}_{\rm 3body} = 1 - \mathcal{B}[K_1(1270) \to K\omega]$ is the BF of the three-body decay of $K_1(1270)$ and $\alpha = \{\mathcal{B}[K_1(1270) \to K^*\pi]/\mathcal{B}[K_1(1270) \to K\rho]\}$. We further determine $\mathcal{B}[D^+ \to \bar{K}_1^0(1270)e^+\nu_e] = (2.27 \pm 0.11_{\rm stat} \pm 0.07_{\rm syst} \pm 0.07_{\rm input}) \times 10^{-3}$ and $\mathcal{B}[D^0 \to K_1^-(1270)e^+\nu_e] = (1.02 \pm 0.06_{\rm stat} \pm 0.06_{\rm syst} \pm 0.03_{\rm input}) \times 10^{-3}$. Our BFs of $D \to \bar{K}_1(1270)e^+\nu_e$ are consistent with the previous measurements [29–32] but with improved precision. The upper limits of $\mathcal{B}[D^+ \to \bar{K}_1^0(1400)e^+\nu_e]$ and $\mathcal{B}[D^0 \to K_1^-(1400)e^+\nu_e]$ are set to be 1.4×10^{-4} and 0.7×10^{-4} at 90% CL, respectively.

TABLE II. Fitted parameters and fit fractions, where the first uncertainties are statistical and the second systematic.

Variable	Value
$r_A(\times 10^{-2})$	$-11.2 \pm 1.0 \pm 0.9$
$r_V(\times 10^{-2})$	$-4.3 \pm 1.0 \pm 2.5$
$f^{D^+}_{\rho K^-}$ (%)	$79.3 \pm 2.0 \pm 25.7$
$f^{D^+}_{\pi\bar{K}^*(892)}$ (%)	$10.9 \pm 1.2 \pm 3.0$
$f^{D^+}_{\bar{K}_1(1400)}$ (%)	< 5
$f^{D^0}_{\rho K^-}$ (%)	$71.8 \pm 2.3 \pm 23.9$
$f^{D^0}_{\pi\bar{K}^*(892)}$ (%)	$19.5 \pm 1.9 \pm 5.2$
$f^{D^0}_{\bar{K}_1(1400)}$ (%)	< 9
$m_{K_1(1270)}$ (MeV/c^2)	$1271 \pm 3 \pm 7$
$\Gamma_{K_1(1270)}$ (MeV)	$168 \pm 10 \pm 20$

An additional binned two-dimensional χ^2 fit is performed on the $\cos\theta_L$ versus $\cos\theta_K$ distributions of the D^+ and D^0 channels simultaneously, to extract the up-down asymmetry $\mathcal{A}'_{\rm ud}$ in the $D \to \bar{K}_1(1270)e^+\nu_e$ decay. This asymmetry relates to the photon polarization λ_γ in $b \to s\gamma$ via $\lambda_\gamma = \frac{4}{3}(\mathcal{A}_{\rm ud}/\mathcal{A}'_{\rm ud})$ [24], where $\mathcal{A}_{\rm ud} = 0.069 \pm 0.017$ is the up-down asymmetry in $B^+ \to K_1(1270)^+(\to K^+\pi^-\pi^+)\gamma$ [28]. The probability density function $f(\cos\theta_L, \cos\theta_K; \mathcal{A}'_{\rm ud}, d_+, d_-)$ is cited from Ref. [58], where $d_{\lambda_W} = |c_{\lambda_w}|^2/|c_0|^2$ is the contribution ratio of $\lambda_w = \pm$ to $\lambda_w = 0$. To keep consistent with the convention in Ref. [28], the direction normal to the K_1 decay plane is defined as $\vec{n} = \vec{p}_{\pi,\rm slow} \times \vec{p}_{\pi,\rm fast}$ instead, and additional mass window $M_{\bar{K}\pi\pi} \in [1.1, 1.3]$ GeV/c^2 is required. The construction of the χ^2 function and the fit projections are described in Appendix C. The fit gives $\mathcal{A}'_{\rm ud} = 0.01 \pm 0.11$, which is consistent with the SM prediction (0.092 ± 0.022). Additionally, the fraction of $\bar{K}_1(1270)$ longitudinal polarization $F_L = |c_0|^2/(|c_0|^2 + |c_+|^2 + |c_-|^2) = 1/(1 + d_+ + d_-)$ is determined to be 0.50 ± 0.04 with statistical uncertainty only, which is consistent with Ref. [31] but with 4 times higher precision. Here, the potential systematic uncertainties are negligible.

The systematic uncertainties in the BF measurements are discussed below. The uncertainty associated with the ST yield $N^{\rm tot}_{\rm ST}$ is estimated to be 0.3% [59]. The efficiencies of tracking, PID, and π^0 reconstruction are studied with $e^+e^- \to \gamma e^+e^-$ and $D\bar{D}$ hadronic decays. The uncertainties are assigned to be 0.5% for tracking or PID for each charged track and 1.0% for each π^0. The uncertainties associated with various cuts are studied with the control samples $D^{+(0)} \to K^0_S\pi^{0(-)}e^+\nu_e$, which are estimated to be 2.0% for D^+ and 4.6% for D^0, respectively. The uncertainties of the $U_{\rm miss}$ fits are estimated to be 0.2% for both D^+ and D^0 channels by changing the fit range and background shapes, as well as varying the peaking background yield. The uncertainties due to the MC model are estimated by varying the parameters in the amplitude model when generating the MC samples. The relative signal efficiency variations are 0.8% and 0.9% for D^+ and D^0, respectively. The uncertainty of final state radiation recovery is assigned to be 0.3% [60]. Combining all individual contributions in quadrature, the overall uncertainties are 3.3% and 5.5% for D^+ and D^0, respectively.

The systematic uncertainties of the amplitude analysis are given below. The uncertainty due to nonsignificant components is estimated by including them into the solution separately. The uncertainty of the radius parameter in the Blatt-Weisskopf factor [48] is estimated by varying it from 3 GeV^{-1} to 2 and 4 GeV^{-1}. The uncertainty due to the line shape of $\bar{K}_1(1270)$ is estimated by using the alternative energy-dependent width $\Gamma(s) \propto (1/\sqrt{s})\int |M_{R\to abc}|^2 {\rm d}\Phi_3$ [55]. The uncertainty associated with the background level is estimated by varying it within its uncertainty. The uncertainty due to parametrization of FFs is estimated by applying alternative modified pole model and parameter series expansion model following $D \to \bar{K}\ell^+\nu_\ell$ [61,62] with detailed results given in Appendix A. The maximum changes on the amplitude fit results are assigned as the corresponding uncertainties. The uncertainty of fit bias, which is caused by the resolution effects as well as imperfect background modeling, is studied via 200 toy MC samples with background included. Amplitude fits are repeated to each sample, and the pull distributions of the fit results are fitted by a Gaussian function. The obtained mean values are assigned as this uncertainty. Detailed systematic uncertainties are given in Ref. [44].

In summary, we have made the first measurements of the hadronic FFs of $D \to \bar{K}_1(1270)$, which are the first in the SL transitions of heavy mesons into axial-vector mesons. We have also presented the improved measurements of the BFs of $D \to \bar{K}_1(1270)e^+\nu_e$ and the first search for $D \to \bar{K}_1(1400)e^+\nu_e$. Figure 3 shows a comparison of the measured FFs and BFs with different theoretical predictions [6–10] as a function of θ_{K_1}. Our r_A, r_V, and $\mathcal{B}[D \to \bar{K}_1(1270)e^+\nu_e]$ are consistent with the 3PSR predictions [7] with $\theta_{K_1} \in (61, 67)°$, and disfavor all other theoretical calculations by more than 5σ. However, our upper limits on $\mathcal{B}[D \to \bar{K}_1(1400)e^+\nu_e]$ disfavor the corresponding 3PSR predictions. More universal theoretical calculations for all four variables are still desired. Additionally, the up-down asymmetry $\mathcal{A}'_{\rm ud}$ is extracted for the first time and no new physics effect is found with the current statistics. Forthcoming larger $B \to \bar{K}_1(1270)\gamma$ [63,64] and $D \to \bar{K}_1(1270)e^+\nu_e$ [65] samples are expected to provide more effective restriction on the right-handed couplings in new physics models.

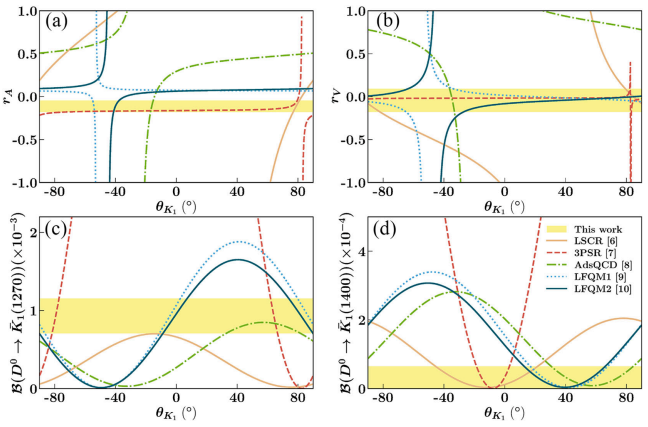

FIG. 3. Comparisons of (a) r_A, (b) r_V, (c) $\mathcal{B}[D^0 \to K(1270)^-e^+\nu_e]$, and (d) $\mathcal{B}[D^0 \to K(1400)^-e^+\nu_e]$ measured in this Letter and predicted by various theoretical approaches as a function of θ_{K_1}. The yellow bands show $\pm 5\sigma$ limit for (a), (b), (c), and the upper limit at 90% CL for (d).

Acknowledgments—The BESIII Collaboration thanks the staff of BEPCII and the IHEP computing center for their strong support. This work is supported in part by National Key R&D Program of China under Contract No. 2023YFA1606000; National Natural Science Foundation of China (NSFC) under Contracts No. 11635010, No. 11735014, No. 11935015, No. 11935016, No. 11935018, No. 12025502, No. 12035009, No. 12035013, No. 12061131003, No. 12192260, No. 12192261, No. 12192262, No. 12192263, No. 12192264, No. 12192265, No. 12221005, No. 12225509, No. 12235017, No. 12361141819; the Chinese Academy of Sciences (CAS) Large-Scale Scientific Facility Program; the CAS Center for Excellence in Particle Physics (CCEPP); Joint Large-Scale Scientific Facility Funds of the NSFC and CAS under Contract No. U2032104, U1832207; CAS under Contract No. YSBR-101; 100 Talents Program of CAS; The Excellent Youth Foundation of Henan Scientific Committee under Contract No. 242300421044; The Institute of Nuclear and Particle Physics (INPAC) and Shanghai Key Laboratory for Particle Physics and Cosmology; Agencia Nacional de Investigación y Desarrollo de Chile (ANID), Chile under Contract No. ANID PIA/APOYO AFB230003; German Research Foundation DFG under Contract No. FOR5327; Istituto Nazionale di Fisica Nucleare, Italy; Knut and Alice Wallenberg Foundation under Contracts No. 2021.0174, No. 2021.0299; Ministry of Development of Turkey under Contract No. DPT2006K-120470; National Research Foundation of Korea under Contract No. NRF-2022R1A2C1092335; National Science and Technology fund of Mongolia; National Science Research and Innovation Fund (NSRF) via the Program Management Unit for Human Resources and Institutional Development, Research and Innovation of Thailand under Contract No. B50G670107; Polish National Science Centre under Contract No. 2019/35/O/ST2/02907; Swedish Research Council under Contract No. 2019.04595; The Swedish Foundation for International Cooperation in Research and Higher Education under Contract No. CH2018-7756; U.S. Department of Energy under Contract No. DE-FG02-05ER41374.

Data availability—The data that support the findings of this Letter are not publicly available upon publication because it is not technically feasible and/or the cost of preparing, depositing, and hosting the data would be prohibitive within the terms of this research project. The data are available from the authors upon reasonable request.

[1] N. Cabibbo, Phys. Rev. Lett. **10**, 531 (1963).
[2] M. Kobayashi and T. Maskawa, Prog. Theor. Phys. **49**, 652 (1973).
[3] Y. Aoki *et al.* (Flavour Lattice Averaging Group), arXiv:2411.04268.
[4] B. C. Ke, J. Koponen, H. B. Li, and Y. Zheng, Annu. Rev. Nucl. Part. Sci. **73**, 285 (2023).
[5] Y. S. Amhis *et al.* (HFLAV Collaboration), Phys. Rev. D **107**, 052008 (2023).
[6] S. Momeni and R. Khosravi, J. Phys. G **46**, 105006 (2019).
[7] R. Khosravi, K. Azizi, and N. Ghahramany, Phys. Rev. D **79**, 036004 (2009).
[8] S. Momeni and M. Saghebfar, Eur. Phys. J. C **82**, 473 (2022).
[9] H. Y. Cheng, C. K. Chua, and C. W. Hwang, Phys. Rev. D **69**, 074025 (2004).
[10] R. C. Verma, J. Phys. G **39**, 025005 (2012); H. Y. Cheng and X. W. Kang, Eur. Phys. J. C **77**, 587 (2017).
[11] Y. J. Shi, J. Zeng, and Z. F. Deng, Phys. Rev. D **109**, 016027 (2024).
[12] M. Suzuki, Phys. Rev. D **47**, 1252 (1993).
[13] F. Divotgey, L. Olbrich, and F. Giacosa, Eur. Phys. J. A **49**, 135 (2013).
[14] H. Hatanaka and K. C. Yang, Phys. Rev. D **77**, 094023 (2008).
[15] H. Y. Cheng, Phys. Lett. B **707**, 116 (2012).
[16] H. G. Blundell, S. Godfrey, and B. Phelps, Phys. Rev. D **53**, 3712 (1996).
[17] A. Tayduganov, E. Kou, and A. Le Yaouanc, Phys. Rev. D **85**, 074011 (2012).
[18] H. J. Lipkin, Phys. Lett. B **72**, 249 (1977).
[19] L. Burakovsky and J. Goldman, Phys. Rev. D **56**, R1368 (1997).
[20] H. Y. Cheng and C. K. Chua, Phys. Rev. D **69**, 094007 (2004).
[21] H. Y. Cheng, Phys. Rev. D **67**, 094007 (2003).
[22] P. F. Guo, D. Wang, and F. S. Yu, Nucl. Phys. Rev. **36**, 125 (2019).
[23] W. Wang, F. S. Yu, and Z. X. Zhao, Phys. Rev. Lett. **125**, 051802 (2020).
[24] L. Bian, L. Sun, and W. Wang, Phys. Rev. D **104**, 053003 (2021).
[25] D. Atwood, M. Gronau, and A. Soni, Phys. Rev. Lett. **79**, 185 (1997).
[26] D. Becirevic, E. Kou, A. Le Yaouanc, and A. Tayduganov, J. High Energy Phys. 08 (2012) 090.
[27] A. Paul and D. M. Straub, J. High Energy Phys. 04 (2017) 027.
[28] R. Aaij *et al.* (LHCb Collaboration), Phys. Rev. Lett. **112**, 161801 (2014).
[29] M. Artuso *et al.* (CLEO Collaboration), Phys. Rev. Lett. **99**, 191801 (2007).
[30] M. Ablikim *et al.* (BESIII Collaboration), Phys. Rev. Lett. **123**, 231801 (2019).
[31] M. Ablikim *et al.* (BESIII Collaboration), Phys. Rev. Lett. **127**, 131801 (2021).
[32] M. Ablikim *et al.* (BESIII Collaboration), J. High Energy Phys. 09 (2024) 089.
[33] M. Ablikim *et al.* (BESIII Collaboration), Chin. Phys. C **48**, 123001 (2024).
[34] Throughout this Letter, the charged-conjugation modes are always implied.

[35] M. Ablikim *et al.* (BESIII Collaboration), Nucl. Instrum. Methods Phys. Res., Sect. A **614**, 345–399 (2010).
[36] K. X. Huang, Z. J. Li, Z. Qian, J. Zhu, H. Y. Li, Y. M. Zhang, S. S. Sun, and Z. Y. You, Nucl. Sci. Tech. **33**, 142 (2022).
[37] S. Agostinelli *et al.* (GEANT4 Collaboration), Nucl. Instrum. Methods Phys. Res., Sect. A **506**, 250 (2003).
[38] S. Jadach, B. F. L. Ward, and Z. Was, Comput. Phys. Commun. **130**, 2602 (2000).
[39] S. Jadach, B. F. L. Ward, and Z. Was, Phys. Rev. D **63**, 113009 (2001).
[40] D. J. Lange, Nucl. Instrum. Methods Phys. Res., Sect. A **462**, 152 (2001).
[41] R. G. Ping, Chin. Phys. C **32**, 599 (2008).
[42] E. Richter-Was, Phys. Lett. B **303**, 163 (1993).
[43] M. Ablikim *et al.* (BESIII Collaboration), Phys. Rev. D **109**, 072003 (2024).
[44] See Supplemental Material at http://link.aps.org/supplemental/10.1103/xj42-xgzf for ST yields and efficiencies, amplitude formulas, and systematic uncertainties for amplitude analysis, which includes Refs. [45–47].
[45] J. G. Korner and G. A. Schuler, Z. Phys. C **46**, 93 (1990).
[46] B. S. Zou and D. V. Bugg, Eur. Phys. J. A **16**, 537 (2003).
[47] I. Adachi *et al.* (*BABAR* and Belle Collaborations), Phys. Rev. D **98**, 112012 (2018).
[48] S. Navas *et al.* (Particle Data Group), Phys. Rev. D **110**, 030001 (2024).
[49] M. Ablikim *et al.* (BESIII Collaboration), Phys. Rev. D **95**, 072010 (2017).
[50] T. Becher and R. J. Hill, Phys. Lett. B **633**, 61 (2006).
[51] D. Becirevic and A. B. Kaidalov, Phys. Lett. B **478**, 417 (2000).
[52] M. Ablikim *et al.* (BESIII Collaboration), Phys. Rev. D **94**, 032001 (2016).
[53] H. Guler *et al.* (Belle Collaboration), Phys. Rev. D **83**, 032005 (2011).
[54] R. Aaij *et al.* (LHCb Collaboration), J. High Energy Phys. 01 (2025) 054.
[55] R. Aaij *et al.* (LHCb Collaboration), Eur. Phys. J. C **78**, 443 (2018).
[56] M. Ablikim *et al.* (BESIII Collaboration), Phys. Rev. D **104**, 032011 (2021).
[57] R. Aaij *et al.* (LHCb Collaboration), J. High Energy Phys. 02 (2019) 126.
[58] Y. L. Fan, X. D. Shi, X. R. Zhou, and L. Sun, Eur. Phys. J. C **81**, 1068 (2021).
[59] M. Ablikim *et al.* (BESIII Collaboration), J. High Energy Phys. 12 (2024) 206.
[60] M. Ablikim *et al.* (BESIII Collaboration), Phys. Rev. D **92**, 072012 (2015).
[61] D. Besson *et al.* (CLEO Collaboration), Phys. Rev. D **80**, 032005 (2009).
[62] M. Ablikim *et al.* (BESIII Collaboration), Phys. Rev. D **110**, 112006 (2024).
[63] L. Aggarwal *et al.* (Belle-II Collaboration), arXiv:2207.06307.
[64] R. Aaij *et al.* (LHCb Collaboration), J. Instrum. **19**, P05065 (2024).
[65] H. Y. Cheng, X. R. Lyu, and Z. Z. Xing, Chin. Phys. Lett. **42**, 010201 (2025).

End Matter

Appendix A: Parametrization of form factors—In principle, the FFs can be expressed in terms of the dispersion relation [50]. Based on that, several parametrizations of FFs are developed for experimental measurements and the following are considered in this Letter. (1) The simplest parametrization is the single pole model $f(q^2) = f(0)/[1 - (q^2/M^2_{\rm pole})]$, where the contributions other than the lowest lying pole are ignored. Because of limited statistics, we take this parametrization for the nominal solution. (2) Another parametrization is known as the modified pole model $f(q^2) = \{f(0)/[1 - (q^2/M^2_{\rm pole})][1 - \beta(q^2/M^2_{\rm pole})]\}$ [51], where the other contributions are included as an effective pole with position $s = (1/\beta)M^2_{\rm pole}$. The current statistics are not sensitive to the additional parameter β, hence we fix it to $\beta = 0.3$ [61] determined in $D \to \bar{K}\ell^+\nu_\ell$. (3) The third parametrization is known as the series expansion model $f(q^2) = [1/P(q^2)\Phi(q^2,t_0)]a_0(t_0)(1+\sum_{k=1}^{\infty} r_k(t_0)[z(q^2,t_0)]^k)$ [50]. This parametrization gives good description to the $D \to \bar{K}\ell^+\nu_\ell$ transition in high precision [62] with $k \leq 1$. Both one- and two-parameter series expansion models are tried. For the two-parameter case, we fix it to $r_1(t_0) = -2.3$ determined in $D \to \bar{K}\ell^+\nu_\ell$ [62].

TABLE III. Fitted r_A and r_V with different parametrizations of FFs, and the change of log-likelihood $\Delta \ln \mathcal{L}$ compared to the single pole model.

Variable	$r_A(\times 10^{-2})$	$r_V(\times 10^{-2})$	$\Delta \ln \mathcal{L}$
Single pole	-11.2 ± 1.0	-4.3 ± 1.0	0.0
Modified pole	-11.3 ± 1.1	-4.8 ± 1.0	-0.4
One-parameter series expansion	-11.2 ± 1.0	-4.2 ± 1.0	$+0.1$
Two-parameter series expansion	-11.2 ± 1.1	-4.5 ± 1.0	-0.2
Uncertainty	0.1	0.5	⋯

Table III summaries the fitted r_A and r_V with different parametrization of FFs. The largest variations are taken as the corresponding systematic uncertainties.

Appendix B: Projections on helicity angles—The projections of the amplitude analysis on the helicity angles in the secondary decay $\bar{K}_1(1270) \to K^-\pi^+\pi^{0(-)}$ are shown in Fig. 4.

Appendix C: Angular fit on $\cos\theta_L$ *vs* $\cos\theta_K$—The distribution function $f(\cos\theta_L, \cos\theta_K; \mathcal{A}'_{\rm ud}, d_+, d_-)$ cited from Ref. [58] is written as

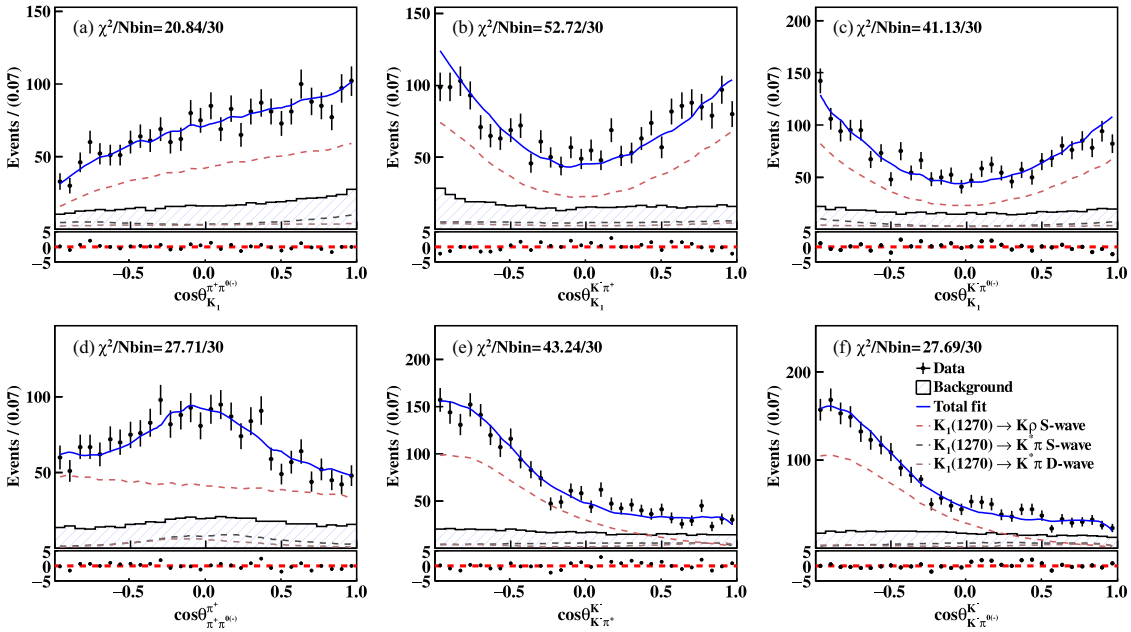

FIG. 4. Projections of the amplitude analysis on the helicity angles (a) $\cos\theta_{K_1}^{\pi^+\pi^{0(-)}}$, (b) $\cos\theta_{K_1}^{K^-\pi^+}$, (c) $\cos\theta_{K_1}^{K^-\pi^{0(-)}}$, (d) $\cos\theta_{\pi^+\pi^{0(-)}}^{\pi^+}$, (e) $\cos\theta_{K^-\pi^+}^{K^-}$, and (f) $\cos\theta_{K^-\pi^{0(-)}}^{K^-}$. The dots with error bars are data, the blue solid curves are the total fits, the dashed curves are the various components, and the blue hatched histograms are the backgrounds. The pull distributions defined as $\chi = (N_{\rm data} - N_{\rm fit})/\sqrt{N_{\rm fit}}$ are shown in the lower plots, where $N_{\rm data}$ and $N_{\rm fit}$ are the data and fit number of events of projections for each bin, respectively.

$$\begin{aligned} f(\cos\theta_K, \cos\theta_l; \mathcal{A}'_{\rm ud}, d_+, d_-) &= (4 + d_+ + d_-)[1 + \cos^2\theta_K \cos^2\theta_l] \\ &+ 2(d_+ - d_-)[1 + \cos^2\theta_K]\cos\theta_l + 2\mathcal{A}'_{\rm ud}(d_+ - d_-)[1 + \cos^2\theta_l]\cos\theta_K \\ &+ 4\mathcal{A}'_{\rm ud}(d_+ + d_-)\cos\theta_K \cos\theta_l - (4 - d_+ - d_-)[\cos^2\theta_K + \cos^2\theta_l]. \end{aligned} \tag{C1}$$

A binned 2D χ^2 fit is performed to extract $\mathcal{A}'_{\rm ud}$, d_+, and d_-. The bin division is 10×10 in the range of $\cos\theta_l \in [-1, 1]$ & $\cos\theta_K \in [-1, 1]$. The χ^2 is defined as

$$\chi^2 = \sum_{i,j} [N_{ij}^{\rm data} - (N_{ij}^{\rm bkg} + N_{ij}^{\rm sig})]^2 / (N_{ij}^{\rm bkg} + N_{ij}^{\rm sig}). \tag{C2}$$

Here, the $N_{ij}^{\rm data}$ and $N_{ij}^{\rm bkg}$ are the number of events of the data and the normalized inclusive MC sample in bin (i, j). The $N_{ij}^{\rm sig}$ is the expected signal number with efficiency considered as

$$\begin{aligned} N_{ij}^{\rm sig}(A'_{\rm ud}, d_+, d_-) = &\frac{\sum_\alpha^{N_{ij}^{\rm un}} \epsilon_\alpha \times f_\alpha(\cos\theta_l, \cos\theta_K; A'_{\rm ud}, d_+, d_-)}{\sum_\alpha^{N^{\rm un}} \epsilon_\alpha \times f_\alpha(\cos\theta_l, \cos\theta_K; A'_{\rm ud}, d_+, d_-)} \\ &\times (N^{\rm data} - N^{\rm bkg}). \end{aligned} \tag{C3}$$

Here, ϵ_α is the binned efficiency determined with signal MC sample as $\epsilon_{\alpha\in(i,j)} = N_{ij}^{\rm rec}/N_{ij}^{\rm tru}$ to take into account detector effects. The $N^{\rm un} = 100\,000$ is the number of random sets $(\cos\theta_l, \cos\theta_K)$ generated uniformly in the range of $\cos\theta_l \in [-1, 1]$ & $\cos\theta_K \in [-1, 1]$ and $N_{ij}^{\rm un}$ indicates the set falls into the bin ij. The simultaneous fit is performed by minimizing $\chi^2_{\rm sum} = \chi^2_{D^+} + \chi^2_{D^0}$. The fit projections are shown in Fig. 5.

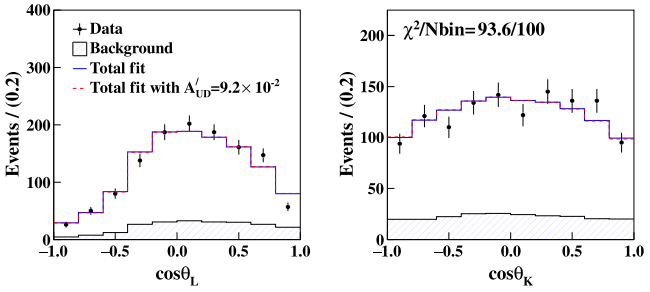

FIG. 5. Fit projections of angular fit on $\cos\theta_l$ (left) and $\cos\theta_K$ (right). The blue curves are the fit results with float $\mathcal{A}'_{\rm ud}$. The red curves are the fit results with the predicted value $\mathcal{A}'_{\rm ud} = 0.092$ as a reference.

M. Ablikim,[1] M. N. Achasov,[4,c] P. Adlarson,[76] X. C. Ai,[81] R. Aliberti,[35] A. Amoroso,[75a,75c] Q. An,[72,58,a] Y. Bai,[57] O. Bakina,[36] Y. Ban,[46,h] H.-R. Bao,[64] V. Batozskaya,[1,44] K. Begzsuren,[32] N. Berger,[35] M. Berlowski,[44] M. Bertani,[28a] D. Bettoni,[29a] F. Bianchi,[75a,75c] E. Bianco,[75a,75c] A. Bortone,[75a,75c] I. Boyko,[36] R. A. Briere,[5] A. Brueggemann,[69] H. Cai,[77] M. H. Cai,[38,k,l] X. Cai,[1,58] A. Calcaterra,[28a] G. F. Cao,[1,64] N. Cao,[1,64] S. A. Cetin,[62a] X. Y. Chai,[46,h] J. F. Chang,[1,58] G. R. Che,[43] Y. Z. Che,[1,58,64] G. Chelkov,[36,b] C. H. Chen,[9] Chao Chen,[55] G. Chen,[1] H. S. Chen,[1,64] H. Y. Chen,[20] M. L. Chen,[1,58,64] S. J. Chen,[42] S. L. Chen,[45] S. M. Chen,[61] T. Chen,[1,64] X. R. Chen,[31,64] X. T. Chen,[1,64] Y. B. Chen,[1,58] Y. Q. Chen,[34] Z. J. Chen,[25,i] Z. K. Chen,[59] S. K. Choi,[10] X. Chu,[12,g] G. Cibinetto,[29a] F. Cossio,[75c] J. J. Cui,[50] H. L. Dai,[1,58] J. P. Dai,[79] A. Dbeyssi,[18] R. E. de Boer,[3] D. Dedovich,[36] C. Q. Deng,[73] Z. Y. Deng,[1] A. Denig,[35] I. Denysenko,[36] M. Destefanis,[75a,75c] F. De Mori,[75a,75c] B. Ding,[67,1] X. X. Ding,[46,h] Y. Ding,[40] Y. Ding,[34] Y. X. Ding,[30] J. Dong,[1,58] L. Y. Dong,[1,64] M. Y. Dong,[1,58,64] X. Dong,[77] M. C. Du,[1] S. X. Du,[12,g] S. X. Du,[81] Y. Y. Duan,[55] Z. H. Duan,[42] P. Egorov,[36,b] G. F. Fan,[42] J. J. Fan,[19] Y. H. Fan,[45] J. Fang,[59] J. Fang,[1,58] S. S. Fang,[1,64] W. X. Fang,[1] Y. Q. Fang,[1,58] R. Farinelli,[29a] L. Fava,[75b,75c] F. Feldbauer,[3] G. Felici,[28a] C. Q. Feng,[72,58] J. H. Feng,[59] Y. T. Feng,[72,58] M. Fritsch,[3] C. D. Fu,[1] J. L. Fu,[64] Y. W. Fu,[1,64] H. Gao,[64] X. B. Gao,[41] Y. N. Gao,[46,h] Y. N. Gao,[19] Y. Y. Gao,[30] Yang Gao,[72,58] S. Garbolino,[75c] I. Garzia,[29a,29b] P. T. Ge,[19] Z. W. Ge,[42] C. Geng,[59] E. M. Gersabeck,[68] A. Gilman,[70] K. Goetzen,[13] J. D. Gong,[34] L. Gong,[40] W. X. Gong,[1,58] W. Gradl,[35] S. Gramigna,[29a,29b] M. Greco,[75a,75c] M. H. Gu,[1,58] Y. T. Gu,[15] C. Y. Guan,[1,64] A. Q. Guo,[31] L. B. Guo,[41] M. J. Guo,[50] R. P. Guo,[49] Y. P. Guo,[12,g] A. Guskov,[36,b] J. Gutierrez,[27] K. L. Han,[64] T. T. Han,[1] F. Hanisch,[3] K. D. Hao,[72,58] X. Q. Hao,[19] F. A. Harris,[66] K. K. He,[55] K. L. He,[1,64] F. H. Heinsius,[3] C. H. Heinz,[35] Y. K. Heng,[1,58,64] C. Herold,[60] T. Holtmann,[3] P. C. Hong,[34] G. Y. Hou,[1,64] X. T. Hou,[1,64] Y. R. Hou,[64] Z. L. Hou,[1] H. M. Hu,[1,64] J. F. Hu,[56,j] Q. P. Hu,[72,58] S. L. Hu,[12,g] T. Hu,[1,58,64] Y. Hu,[1] Z. M. Hu,[59] G. S. Huang,[72,58] K. X. Huang,[59] L. Q. Huang,[31,64] P. Huang,[42] X. T. Huang,[50] Y. P. Huang,[1] Y. S. Huang,[59] T. Hussain,[74] N. Hüsken,[35] N. in der Wiesche,[69] J. Jackson,[27] S. Janchiv,[32] Q. Ji,[1] Q. P. Ji,[19] W. Ji,[1,64] X. B. Ji,[1,64] X. L. Ji,[1,58] Y. Y. Ji,[50] Z. K. Jia,[72,58] D. Jiang,[1,64] H. B. Jiang,[77] P. C. Jiang,[46,h] S. J. Jiang,[9] T. J. Jiang,[16] X. S. Jiang,[1,58,64] Y. Jiang,[64] J. B. Jiao,[50] J. K. Jiao,[34] Z. Jiao,[23] S. Jin,[42] Y. Jin,[67] M. Q. Jing,[1,64] X. M. Jing,[64] T. Johansson,[76] S. Kabana,[33] N. Kalantar-Nayestanaki,[65] X. L. Kang,[9] X. S. Kang,[40] M. Kavatsyuk,[65] B. C. Ke,[81] V. Khachatryan,[27] A. Khoukaz,[69] R. Kiuchi,[1] O. B. Kolcu,[62a] B. Kopf,[3] M. Kuessner,[3] X. Kui,[1,64] N. Kumar,[26] A. Kupsc,[44,76] W. Kühn,[37] Q. Lan,[73] W. N. Lan,[19] T. T. Lei,[72,58] M. Lellmann,[35] T. Lenz,[35] C. Li,[47] C. Li,[43] C. H. Li,[39] C. K. Li,[20] Cheng Li,[72,58] D. M. Li,[81] F. Li,[1,58] G. Li,[1] H. B. Li,[1,64] H. J. Li,[19] H. N. Li,[56,j] Hui Li,[43] J. R. Li,[61] J. S. Li,[59] K. Li,[1] K. L. Li,[19] K. L. Li,[38,k,l] L. J. Li,[1,64] Lei Li,[48] M. H. Li,[43] M. R. Li,[1,64] P. L. Li,[64] P. R. Li,[38,k,l] Q. M. Li,[1,64] Q. X. Li,[50] R. Li,[17,31] T. Li,[50] T. Y. Li,[43] W. D. Li,[1,64] W. G. Li,[1,a] X. Li,[1,64] X. H. Li,[72,58] X. L. Li,[50] X. Y. Li,[1,8] X. Z. Li,[59] Y. Li,[19] Y. G. Li,[46,h] Y. P. Li,[34] Z. J. Li,[59] Z. Y. Li,[79] C. Liang,[42] H. Liang,[72,58] Y. F. Liang,[54] Y. T. Liang,[31,64] G. R. Liao,[14] L. B. Liao,[59] M. H. Liao,[59] Y. P. Liao,[1,64] J. Libby,[26] A. Limphirat,[60] C. C. Lin,[55] C. X. Lin,[64] D. X. Lin,[31,64] L. Q. Lin,[39] T. Lin,[1] B. J. Liu,[1] B. X. Liu,[77] C. Liu,[34] C. X. Liu,[1] F. Liu,[1] F. H. Liu,[53] Feng Liu,[6] G. M. Liu,[56,j] H. Liu,[38,k,l] H. B. Liu,[15] H. H. Liu,[1] H. M. Liu,[1,64] Huihui Liu,[21] J. B. Liu,[72,58] J. J. Liu,[20] K. Liu,[38,k,l] K. Liu,[73] K. Y. Liu,[40] Ke Liu,[22] L. Liu,[72,58] L. C. Liu,[43] Lu Liu,[43] P. L. Liu,[1] Q. Liu,[64] S. B. Liu,[72,58] T. Liu,[12,g] W. K. Liu,[43] W. M. Liu,[72,58] W. T. Liu,[39] X. Liu,[39] X. Liu,[38,k,l] X. Y. Liu,[77] Y. Liu,[38,k,l] Y. Liu,[81] Y. Liu,[81] Y. B. Liu,[43] Z. A. Liu,[1,58,64] Z. D. Liu,[9] Z. Q. Liu,[50] X. C. Lou,[1,58,64] F. X. Lu,[59] H. J. Lu,[23] J. G. Lu,[1,58] Y. Lu,[7] Y. H. Lu,[1,64] Y. P. Lu,[1,58] Z. H. Lu,[1,64] C. L. Luo,[41] J. R. Luo,[59] J. S. Luo,[1,64] M. X. Luo,[80] T. Luo,[12,g] X. L. Luo,[1,58] Z. Y. Lv,[22] X. R. Lyu,[64,p] Y. F. Lyu,[43] Y. H. Lyu,[81] F. C. Ma,[40] H. Ma,[79] H. L. Ma,[1] J. L. Ma,[1,64] L. L. Ma,[50] L. R. Ma,[67] Q. M. Ma,[1] R. Q. Ma,[1,64] R. Y. Ma,[19] T. Ma,[72,58] X. T. Ma,[1,64] X. Y. Ma,[1,58] Y. M. Ma,[31] F. E. Maas,[18] I. MacKay,[70] M. Maggiora,[75a,75c] S. Malde,[70] Y. J. Mao,[46,h] Z. P. Mao,[1] S. Marcello,[75a,75c] F. M. Melendi,[29a,29b] Y. H. Meng,[64] Z. X. Meng,[67] J. G. Messchendorp,[13,65] G. Mezzadri,[29a] H. Miao,[1,64] T. J. Min,[42] R. E. Mitchell,[27] X. H. Mo,[1,58,64] B. Moses,[27] N. Yu. Muchnoi,[4,c] J. Muskalla,[35] Y. Nefedov,[36] F. Nerling,[18,e] L. S. Nie,[20] I. B. Nikolaev,[4,c] Z. Ning,[1,58] S. Nisar,[11,m] Q. L. Niu,[38,k,l] W. D. Niu,[12,g] S. L. Olsen,[10,64] Q. Ouyang,[1,58,64] S. Pacetti,[28b,28c] X. Pan,[55] Y. Pan,[57] A. Pathak,[10] Y. P. Pei,[72,58] M. Pelizaeus,[3] H. P. Peng,[72,58] Y. Y. Peng,[38,k,l] K. Peters,[13,e] J. L. Ping,[41] R. G. Ping,[1,64] S. Plura,[35] V. Prasad,[33] F. Z. Qi,[1] H. R. Qi,[61] M. Qi,[42] S. Qian,[1,58] W. B. Qian,[64] C. F. Qiao,[64] J. H. Qiao,[19] J. J. Qin,[73] J. L. Qin,[55] L. Q. Qin,[14] L. Y. Qin,[72,58] P. B. Qin,[73] X. P. Qin,[12,g] X. S. Qin,[50] Z. H. Qin,[1,58] J. F. Qiu,[1] Z. H. Qu,[73] C. F. Redmer,[35] A. Rivetti,[75c] M. Rolo,[75c] G. Rong,[1,64] S. S. Rong,[1,64] F. Rosini,[28b,28c] Ch. Rosner,[18] M. Q. Ruan,[1,58] N. Salone,[44] A. Sarantsev,[36,d] Y. Schelhaas,[35] K. Schoenning,[76] M. Scodeggio,[29a] K. Y. Shan,[12,g] W. Shan,[24] X. Y. Shan,[72,58] Z. J. Shang,[38,k,l] J. F. Shangguan,[16] L. G. Shao,[1,64] M. Shao,[72,58] C. P. Shen,[12,g] H. F. Shen,[1,8] W. H. Shen,[64] X. Y. Shen,[1,64] B. A. Shi,[64] H. Shi,[72,58] J. L. Shi,[12,g] J. Y. Shi,[1] S. Y. Shi,[73] X. Shi,[1,58] H. L. Song,[72,58] J. J. Song,[19] T. Z. Song,[59] W. M. Song,[34,1] Y. X. Song,[46,h,n] S. Sosio,[75a,75c] S. Spataro,[75a,75c] F. Stieler,[35] S. S. Su,[40] Y. J. Su,[64] G. B. Sun,[77] G. X. Sun,[1] H. Sun,[64] H. K. Sun,[1] J. F. Sun,[19] K. Sun,[61]

L. Sun,[77] S. S. Sun,[1,64] T. Sun,[51,f] Y. C. Sun,[77] Y. H. Sun,[30] Y. J. Sun,[72,58] Y. Z. Sun,[1] Z. Q. Sun,[1,64] Z. T. Sun,[50] C. J. Tang,[54] G. Y. Tang,[1] J. Tang,[59] L. F. Tang,[39] M. Tang,[72,58] Y. A. Tang,[77] L. Y. Tao,[73] M. Tat,[70] J. X. Teng,[72,58] J. Y. Tian,[72,58] W. H. Tian,[59] Y. Tian,[31] Z. F. Tian,[77] I. Uman,[62b] B. Wang,[1] B. Wang,[59] Bo Wang,[72,58] C. Wang,[19] Cong Wang,[22] D. Y. Wang,[46,h] H. J. Wang,[38,k,l] J. J. Wang,[77] K. Wang,[1,58] L. L. Wang,[1] L. W. Wang,[34] M. Wang,[72,58] M. Wang,[50] N. Y. Wang,[64] S. Wang,[12,g] T. Wang,[12,g] T. J. Wang,[43] W. Wang,[59] W. Wang,[73] W. P. Wang,[35,58.72,o] X. Wang,[46,h] X. F. Wang,[38,k,l] X. J. Wang,[39] X. L. Wang,[12,g] X. N. Wang,[1] Y. Wang,[61] Y. D. Wang,[45] Y. F. Wang,[1,58,64] Y. H. Wang,[38,k,l] Y. L. Wang,[19] Y. N. Wang,[77] Y. Q. Wang,[1] Yaqian Wang,[17] Yi Wang,[61] Yuan Wang,[17,31] Z. Wang,[1,58] Z. L. Wang,[73] Z. L. Wang,[2] Z. Q. Wang,[12,g] Z. Y. Wang,[1,64] D. H. Wei,[14] H. R. Wei,[43] F. Weidner,[69] S. P. Wen,[1] Y. R. Wen,[39] U. Wiedner,[3] G. Wilkinson,[70] M. Wolke,[76] C. Wu,[39] J. F. Wu,[1,8] L. H. Wu,[1] L. J. Wu,[1,64] Lianjie Wu,[19] S. G. Wu,[1,64] S. M. Wu,[64] X. Wu,[12,g] X. H. Wu,[34] Y. J. Wu,[31] Z. Wu,[1,58] L. Xia,[72,58] X. M. Xian,[39] B. H. Xiang,[1,64] T. Xiang,[46,h] D. Xiao,[38,k,l] G. Y. Xiao,[42] H. Xiao,[73] Y. L. Xiao,[12,g] Z. J. Xiao,[41] C. Xie,[42] K. J. Xie,[1,64] X. H. Xie,[46,h] Y. Xie,[50] Y. G. Xie,[1,58] Y. H. Xie,[6] Z. P. Xie,[72,58] T. Y. Xing,[1,64] C. F. Xu,[1,64] C. J. Xu,[59] G. F. Xu,[1] H. Y. Xu,[2] H. Y. Xu,[67,2] M. Xu,[72,58] Q. J. Xu,[16] Q. N. Xu,[30] T. D. Xu,[73] W. L. Xu,[67] X. P. Xu,[55] Y. Xu,[12,g] Y. Xu,[40] Y. C. Xu,[78] Z. S. Xu,[64] H. Y. Yan,[39] L. Yan,[12,g] W. B. Yan,[72,58] W. C. Yan,[81] W. P. Yan,[19] X. Q. Yan,[1,64] H. J. Yang,[51,f] H. L. Yang,[34] H. X. Yang,[1] J. H. Yang,[42] R. J. Yang,[19] T. Yang,[1] Y. Yang,[12,g] Y. F. Yang,[43] Y. H. Yang,[42] Y. Q. Yang,[9] Y. X. Yang,[1,64] Y. Z. Yang,[19] M. Ye,[1,58] M. H. Ye,[8] Z. J. Ye,[56,j] Junhao Yin,[43] Z. Y. You,[59] B. X. Yu,[1,58,64] C. X. Yu,[43] G. Yu,[13] J. S. Yu,[25,i] M. C. Yu,[40] T. Yu,[73] X. D. Yu,[46,h] Y. C. Yu,[81] C. Z. Yuan,[1,64] H. Yuan,[1,64] J. Yuan,[45] J. Yuan,[34] L. Yuan,[2] S. C. Yuan,[1,64] Y. Yuan,[1,64] Z. Y. Yuan,[59] C. X. Yue,[39] Ying Yue,[19] A. A. Zafar,[74] S. H. Zeng,[63] X. Zeng,[12,g] Y. Zeng,[25,i] Y. J. Zeng,[59] Y. J. Zeng,[1,64] X. Y. Zhai,[34] Y. H. Zhan,[59] A. Q. Zhang,[1,64] B. L. Zhang,[1,64] B. X. Zhang,[1] D. H. Zhang,[43] G. Y. Zhang,[1,64] G. Y. Zhang,[19] H. Zhang,[72,58] H. Zhang,[81] H. C. Zhang,[1,58,64] H. H. Zhang,[59] H. Q. Zhang,[1,58,64] H. R. Zhang,[72,58] H. Y. Zhang,[1,58] J. Zhang,[81] J. Zhang,[59] J. J. Zhang,[52] J. L. Zhang,[20] J. Q. Zhang,[41] J. S. Zhang,[12,g] J. W. Zhang,[1,58,64] J. X. Zhang,[38,k,l] J. Y. Zhang,[1] J. Z. Zhang,[1,64] Jianyu Zhang,[64] L. M. Zhang,[61] Lei Zhang,[42] N. Zhang,[81] P. Zhang,[1,64] Q. Zhang,[19] Q. Y. Zhang,[34] R. Y. Zhang,[38,k,l] S. H. Zhang,[1,64] Shulei Zhang,[25,i] X. M. Zhang,[1] X. Y. Zhang,[40] X. Y. Zhang,[50] Y. Zhang,[1] Y. Zhang,[73] Y. T. Zhang,[81] Y. H. Zhang,[1,58] Y. M. Zhang,[39] Z. D. Zhang,[1] Z. H. Zhang,[1] Z. L. Zhang,[34] Z. L. Zhang,[55] Z. X. Zhang,[19] Z. Y. Zhang,[43] Z. Y. Zhang,[77] Z. Z. Zhang,[45] Zh. Zh. Zhang,[19] G. Zhao,[1] J. Y. Zhao,[1,64] J. Z. Zhao,[1,58] L. Zhao,[1] Lei Zhao,[72,58] M. G. Zhao,[43] N. Zhao,[79] R. P. Zhao,[64] S. J. Zhao,[81] Y. B. Zhao,[1,58] Y. L. Zhao,[55] Y. X. Zhao,[31,64] Z. G. Zhao,[72,58] A. Zhemchugov,[36,b] B. Zheng,[73] B. M. Zheng,[34] J. P. Zheng,[1,58] W. J. Zheng,[1,64] X. R. Zheng,[19] Y. H. Zheng,[64,p] B. Zhong,[41] X. Zhong,[59] H. Zhou,[35,50,o] J. Q. Zhou,[34] J. Y. Zhou,[34] S. Zhou,[6] X. Zhou,[77] X. K. Zhou,[6] X. R. Zhou,[72,58] X. Y. Zhou,[39] Y. Z. Zhou,[12,g] Z. C. Zhou,[20] A. N. Zhu,[64] J. Zhu,[43] K. Zhu,[1] K. J. Zhu,[1,58,64] K. S. Zhu,[12,g] L. Zhu,[34] L. X. Zhu,[64] S. H. Zhu,[71] T. J. Zhu,[12,g] W. D. Zhu,[12,g] W. D. Zhu,[41] W. J. Zhu,[1] W. Z. Zhu,[19] Y. C. Zhu,[72,58] Z. A. Zhu,[1,64] X. Y. Zhuang,[43] J. H. Zou,[1] and J. Zu[72,58]

(BESIII Collaboration)

[1]*Institute of High Energy Physics, Beijing 100049, People's Republic of China*
[2]*Beihang University, Beijing 100191, People's Republic of China*
[3]*Bochum Ruhr-University, D-44780 Bochum, Germany*
[4]*Budker Institute of Nuclear Physics SB RAS (BINP), Novosibirsk 630090, Russia*
[5]*Carnegie Mellon University, Pittsburgh, Pennsylvania 15213, USA*
[6]*Central China Normal University, Wuhan 430079, People's Republic of China*
[7]*Central South University, Changsha 410083, People's Republic of China*
[8]*China Center of Advanced Science and Technology, Beijing 100190, People's Republic of China*
[9]*China University of Geosciences, Wuhan 430074, People's Republic of China*
[10]*Chung-Ang University, Seoul, 06974, Republic of Korea*
[11]*COMSATS University Islamabad, Lahore Campus, Defence Road, Off Raiwind Road, 54000 Lahore, Pakistan*
[12]*Fudan University, Shanghai 200433, People's Republic of China*
[13]*GSI Helmholtzcentre for Heavy Ion Research GmbH, D-64291 Darmstadt, Germany*
[14]*Guangxi Normal University, Guilin 541004, People's Republic of China*
[15]*Guangxi University, Nanning 530004, People's Republic of China*
[16]*Hangzhou Normal University, Hangzhou 310036, People's Republic of China*
[17]*Hebei University, Baoding 071002, People's Republic of China*
[18]*Helmholtz Institute Mainz, Staudinger Weg 18, D-55099 Mainz, Germany*
[19]*Henan Normal University, Xinxiang 453007, People's Republic of China*

[20]Henan University, Kaifeng 475004, People's Republic of China
[21]Henan University of Science and Technology, Luoyang 471003, People's Republic of China
[22]Henan University of Technology, Zhengzhou 450001, People's Republic of China
[23]Huangshan College, Huangshan 245000, People's Republic of China
[24]Hunan Normal University, Changsha 410081, People's Republic of China
[25]Hunan University, Changsha 410082, People's Republic of China
[26]Indian Institute of Technology Madras, Chennai 600036, India
[27]Indiana University, Bloomington, Indiana 47405, USA
[28a]INFN Laboratori Nazionali di Frascati, INFN Laboratori Nazionali di Frascati, I-00044, Frascati, Italy
[28b]INFN Sezione di Perugia, I-06100, Perugia, Italy
[28c]University of Perugia, I-06100, Perugia, Italy
[29a]INFN Sezione di Ferrara, INFN Sezione di Ferrara, I-44122, Ferrara, Italy
[29b]University of Ferrara, I-44122, Ferrara, Italy
[30]Inner Mongolia University, Hohhot 010021, People's Republic of China
[31]Institute of Modern Physics, Lanzhou 730000, People's Republic of China
[32]Institute of Physics and Technology, Peace Avenue 54B, Ulaanbaatar 13330, Mongolia
[33]Instituto de Alta Investigación, Universidad de Tarapacá, Casilla 7D, Arica 1000000, Chile
[34]Jilin University, Changchun 130012, People's Republic of China
[35]Johannes Gutenberg University of Mainz, Johann-Joachim-Becher-Weg 45, D-55099 Mainz, Germany
[36]Joint Institute for Nuclear Research, 141980 Dubna, Moscow region, Russia
[37]Justus-Liebig-Universitaet Giessen, II. Physikalisches Institut, Heinrich-Buff-Ring 16, D-35392 Giessen, Germany
[38]Lanzhou University, Lanzhou 730000, People's Republic of China
[39]Liaoning Normal University, Dalian 116029, People's Republic of China
[40]Liaoning University, Shenyang 110036, People's Republic of China
[41]Nanjing Normal University, Nanjing 210023, People's Republic of China
[42]Nanjing University, Nanjing 210093, People's Republic of China
[43]Nankai University, Tianjin 300071, People's Republic of China
[44]National Centre for Nuclear Research, Warsaw 02-093, Poland
[45]North China Electric Power University, Beijing 102206, People's Republic of China
[46]Peking University, Beijing 100871, People's Republic of China
[47]Qufu Normal University, Qufu 273165, People's Republic of China
[48]Renmin University of China, Beijing 100872, People's Republic of China
[49]Shandong Normal University, Jinan 250014, People's Republic of China
[50]Shandong University, Jinan 250100, People's Republic of China
[51]Shanghai Jiao Tong University, Shanghai 200240, People's Republic of China
[52]Shanxi Normal University, Linfen 041004, People's Republic of China
[53]Shanxi University, Taiyuan 030006, People's Republic of China
[54]Sichuan University, Chengdu 610064, People's Republic of China
[55]Soochow University, Suzhou 215006, People's Republic of China
[56]South China Normal University, Guangzhou 510006, People's Republic of China
[57]Southeast University, Nanjing 211100, People's Republic of China
[58]State Key Laboratory of Particle Detection and Electronics, Beijing 100049, Hefei 230026, People's Republic of China
[59]Sun Yat-Sen University, Guangzhou 510275, People's Republic of China
[60]Suranaree University of Technology, University Avenue 111, Nakhon Ratchasima 30000, Thailand
[61]Tsinghua University, Beijing 100084, People's Republic of China
[62a]Turkish Accelerator Center Particle Factory Group, Istinye University, 34010, Istanbul, Turkey
[62b]Near East University, Nicosia, North Cyprus, 99138, Mersin 10, Turkey
[63]University of Bristol, H H Wills Physics Laboratory, Tyndall Avenue, Bristol, BS8 1TL, United Kingdom
[64]University of Chinese Academy of Sciences, Beijing 100049, People's Republic of China
[65]University of Groningen, NL-9747 AA Groningen, The Netherlands
[66]University of Hawaii, Honolulu, Hawaii 96822, USA
[67]University of Jinan, Jinan 250022, People's Republic of China
[68]University of Manchester, Oxford Road, Manchester M13 9PL, United Kingdom
[69]University of Muenster, Wilhelm-Klemm-Strasse 9, 48149 Muenster, Germany
[70]University of Oxford, Keble Road, Oxford OX13RH, United Kingdom
[71]University of Science and Technology Liaoning, Anshan 114051, People's Republic of China
[72]University of Science and Technology of China, Hefei 230026, People's Republic of China
[73]University of South China, Hengyang 421001, People's Republic of China
[74]University of the Punjab, Lahore-54590, Pakistan
[75a]University of Turin and INFN, University of Turin, I-10125, Turin, Italy

[75b]University of Eastern Piedmont, I-15121, Alessandria, Italy
[75c]INFN, I-10125, Turin, Italy
[76]Uppsala University, Box 516, SE-75120 Uppsala, Sweden
[77]Wuhan University, Wuhan 430072, People's Republic of China
[78]Yantai University, Yantai 264005, People's Republic of China
[79]Yunnan University, Kunming 650500, People's Republic of China
[80]Zhejiang University, Hangzhou 310027, People's Republic of China
[81]Zhengzhou University, Zhengzhou 450001, People's Republic of China

[a]Deceased.
[b]Also at the Moscow Institute of Physics and Technology, Moscow 141700, Russia.
[c]Also at the Novosibirsk State University, Novosibirsk, 630090, Russia.
[d]Also at the NRC "Kurchatov Institute", PNPI, 188300, Gatchina, Russia.
[e]Also at Goethe University Frankfurt, 60323 Frankfurt am Main, Germany.
[f]Also at Key Laboratory for Particle Physics, Astrophysics and Cosmology, Ministry of Education; Shanghai Key Laboratory for Particle Physics and Cosmology; Institute of Nuclear and Particle Physics, Shanghai 200240, People's Republic of China.
[g]Also at Key Laboratory of Nuclear Physics and Ion-beam Application (MOE) and Institute of Modern Physics, Fudan University, Shanghai 200443, People's Republic of China.
[h]Also at State Key Laboratory of Nuclear Physics and Technology, Peking University, Beijing 100871, People's Republic of China.
[i]Also at School of Physics and Electronics, Hunan University, Changsha 410082, China.
[j]Also at Guangdong Provincial Key Laboratory of Nuclear Science, Institute of Quantum Matter, South China Normal University, Guangzhou 510006, China.
[k]Also at MOE Frontiers Science Center for Rare Isotopes, Lanzhou University, Lanzhou 730000, People's Republic of China.
[l]Also at Lanzhou Center for Theoretical Physics, Lanzhou University, Lanzhou 730000, People's Republic of China.
[m]Also at the Department of Mathematical Sciences, IBA, Karachi 75270, Pakistan.
[n]Also at Ecole Polytechnique Federale de Lausanne (EPFL), CH-1015 Lausanne, Switzerland.
[o]Also at Helmholtz Institute Mainz, Staudinger Weg 18, D-55099 Mainz, Germany.
[p]Also at Hangzhou Institute for Advanced Study, University of Chinese Academy of Sciences, Hangzhou 310024, China.